Available online at www.sciencedirect.com
SCIENCE DIRECT®
Developmental Biology xx (2004) xxx–xxx
DEVELOPMENTAL BIOLOGY
www.elsevier.com/locate/ydbio

Genomes & Developmental Control

Global analysis of genes differentially expressed in branching and non-branching regions of the mouse embryonic lung

Jining Lü, Jun Qian, Konstantin I. Izvolsky, Wellington V. Cardoso*

Pulmonary Center, Boston University School of Medicine, Boston, MA 02118, USA

Received for publication 25 March 2004, revised 18 May 2004, accepted 25 May 2004

Abstract

During development, the proximal and distal regions of respiratory tract undergo distinct processes that ultimately give rise to conducting airways and alveoli. To gain insights into the genetic pathways differentially activated in these regions when branching morphogenesis is initiating, we characterized their transcriptional profiles in murine rudiments isolated at embryonic (E) day 11.5. By using oligonucleotide microarrays, we identified 83 and 128 genes preferentially expressed in branching and non-branching regions, respectively. The majority of these genes (85%) had not been previously described in the lung, or in other organs. We report restricted expression patterns of 22 of these genes were by in situ hybridization. Among them in the lung potential components of the Wnt, TGF beta, FGF and retinoid pathways identified in other systems, and uncharacterized genes, such as translocases, small GTPases and splicing factors. In addition, we provide a more detailed analysis of the expression pattern and regulation of a representative gene from the distal (*transforming growth factor*, *beta induced*) and proximal (*WW domain-containing protein 2*) regions. Our data suggest that these genes may regulate focal developmental events specific of each of these regions during respiratory tract formation.

Keywords: Lung development; Microarrays; Branching morphogenesis; Respiratory tract; Growth factors; TGF beta; *Tgfbi*; *Wwp2*; Ubiquitination; Retinoic acid

Introduction

Development of the respiratory tract involves formation of the tracheobronchial tree and the alveoli; for most species this process spans the embryonic (E) and postnatal periods of life. In mice, primary lung buds and the tracheal primordium emerge independently from the primitive foregut at E9.5. Secondary lung buds appear a day later, and by E11–11.5 they branch to give rise to multiple generations of airways. Concurrently, both epithelial and mesenchymal components of these airways undergo proximal–distal (P–D) differentiation. Proximal regions will form the conducting airways, while the distal regions of the branching tubules will generate the future alveoli (reviewed in Cardoso, 2001; Hogan, 1999).

Tissue recombination experiments in embryonic mouse or rat models have shown that distal lung mesenchyme is able to induce budding and distal gene expression in the developing proximal epithelium (Ohtsuka et al., 2001; Shannon et al., 1998; Wessells, 1970). Differences in the morphogenetic potential of proximal and distal regions of the respiratory tract are evident from the earliest developmental stages. These ultimately reflect differences in the repertoire of signaling molecules present in epithelial and mesenchymal cells along the developing respiratory tract.

There is evidence that during early branching morphogenesis a distal signaling network is established in the E11–12 mouse lung to maintain proper growth and proximal–distal differentiation. For example, distal epithelial buds require local signaling by mesenchymal fibroblast growth factor *Fgf10* for proper induction, while epithelial sonic hedgehog (*Shh*) and bone morphogenetic protein-4 (*Bmp4*) act as negative regulators of this process (reviewed in Cardoso, 2001; Hogan, 1999). By contrast, the proximal non-branching region (main bronchi and trachea) is considered to be morphogenetically less active, proliferating less and starting cellular differentiation earlier (Mollard and Dziadek, 1998). Sites where the proximal mesenchyme will give rise to tracheal cartilage primordia can be identified

* Corresponding author. Pulmonary Center, Boston University School of Medicine, 80 East Concord Street, R-304, Boston, MA 02118. Fax: +1-617-536-8093.
E-mail address: wcardoso@lung.bumc.bu.edu (W.V. Cardoso).

0012-1606/$ - see front matter © 2004 Elsevier Inc. All rights reserved.
doi:10.1016/j.ydbio.2004.05.035

already at E11.5 by local expression of retinoic acid receptor gamma (*Rarγ*), a critical regulator of this process (Mollard et al., 2000b). In addition to regionally expressed regulatory molecules, extracellular matrix (ECM), cell adhesion molecules and even structural molecules are also part of local networks that influence local cellular behavior. Identifying global patterns of gene expression in proximal and distal regions is critical to understand how these differences in cellular behavior and phenotypes arise.

Recently, genome-wide discovery tools in combination with large scale in situ hybridization screen have been used to identify genes expressed in a temporal and spatial-specific fashion in a variety of developmental processes (Butler et al., 2003; Stathopoulos et al., 2002; White et al., 1999). Similar approaches have been used to examine expression profiles during lung development. One of these studies examined whole lungs at different developmental stages (Mariani et al., 2002), while others have focused on genes expressed are an individual germ layer (Liu and Hogan, 2002) or reported a particular regionally expressed gene (Lin and Shannon, 2002).

Here, we used oligonucleotide microarrays to characterize the transcriptional profile of proximal and distal regions of the mouse respiratory tract at E11.5, when branching morphogenesis is initiating. We compared two regions with largely different morphogenetic potentials to gain insights into the pathways that potentially distinguish proximal non-branching from the distal branching region. We provide a complete list of the microarray data, which show little overlap with previously published data. We report the spatial distribution of 22 previously uncharacterized genes. We show that the proximal region is enriched for genes encoding components of the RA pathway, ECM molecules that favor morphogenetic stabilization, including various procollagen genes and SRY-box transcription factors. In the distal region we found potential components of the Wnt, TGF beta and FGF signaling and other pathways reported elsewhere, but not in the lung. Some of these genes, such as translocases and splicing factors, were highly specific for the distal mesenchyme. From this survey we selected a representative distal (*transforming growth factor, beta induced*) and a proximal (*WW domain-containing protein* 2) gene for further analysis because of their unique expression pattern, which suggested a role in regulating specific events locally.

Material and methods

Lung dissection, RNA isolation, labeling and microarray hybridization

Lungs and lower third of trachea were dissected from the E11.5 CD1 mouse embryos. Branching and non-branching regions of the lung were separated as illustrated in Fig. 1. Both right and left lungs were included for the analysis of the branching region. Total RNA from these samples was isolated using RNeasy (Qiagen) and then subjected to labeling and hybridization using the Affymetrix kit according to the manufacturer's manual.

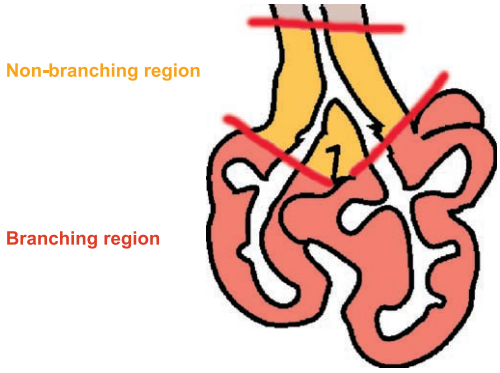

Fig. 1. Diagram illustrates the strategy for sampling of the respiratory tract of E11.5 mouse. The branching region consisted of the right and left lung. Non-branching region included the main bronchi and the lower third of the trachea.

Microarray data analysis

Three arrays (Affymetrix, MG-U74v2 set) were used per each experimental condition. A single weighted mean expression level for each gene along with a detection *P* value (which indicates whether the transcript was reliably detected) was derived using Microarray Suite 5.0 software (Affymetrix, Santa Clara, CA). We scaled the data from each array (target intensity of 500) to normalize the results for inter-array comparisons. The list of genes on this array is available at http://www.affymetrix.com/analysis/download_center.affx. All data from our microarray experiments have been deposited in NCBI's Gene Expression Omnibus; the accession numbers for the samples are: GSM23483, GSM23484, GSM23485, GSM23486, GSM23487, GSM23488.

Each array's scanned image was examined for significant artifacts and the bacterial genes spiked into the hybridization mix had a detection *P* value below 0.05 (called present). In addition, several quality control metrics were assessed on each array. Background signals were within the recommendation limit (less than 100). The scaling factors used to normalize the target value ranged from 0.71 to 1.38 (within 4-fold standard limit). The 3′/5′ ratios of *Gapdh* and beta-actin ranged from 0.86 to1.75 (lower than the four fold standard limit). Genes with detection *P* values greater than 0.05 (called absent) in all six samples were eliminated from our analysis (55% in our case). A Student's *t* test was performed to identify genes differentially expressed between regions. Genes were considered differentially expressed if their fold change (FC) was greater than 1.75 with *P* value (on Student's *t* test) lower than 0.05. This combined statistical and fold change threshold helped us to focus on those genes with most significant changes and excluded potential artificial differences that could arise from low level or undetectable level gene expression in all our samples. The GoMiner

software (Fish Exact *T* test, http://discover.nci.nih.gov/gominer/) (Zeeberg et al., 2003) was used for statistical measure of representation of gene categories enriched in either the branching or non-branching regions. The list for all genes on the chip (Affymetrix, MG-U74v2 set) was input as the query gene file and each of the preferential expression gene list as the query changed gene file. All the information for three different categories in GO (Biological Process, Molecular Function and Cellular Component) was downloaded as Excel files. Categories with *P* value lower than 0.01 were selected for analysis, while the redundant and some subcategories were removed.

Lung organ culture

For the lung organ cultures, E11–12 lungs from CD1 mice, or in some experiments, from *RARE lacZ* transgenic mice (Rossant et al., 1991) were dissected and placed onto MF-Millipore membrane filters (Whatman), on the top of a metal mesh on tissue culture dish, and cultured in BGjb medium (Sigma 20 mg/100 ml of ascorbic acid, 1% of inactivated fetal calf serum and 50 units/μg penicillin/streptomycin). For some experiments, TGFβ1 (human recombinant, 10–50 ng/ml, R&D system), retinoic acid (10^{-6} or 10^{-5} M, Sigma) or BMS493 (10^{-6} M, Bristol-Myers-Squibb) were added to the medium at the beginning of the culture, as previously described (Malpel et al., 2000; Mollard et al., 2000a; Serra et al., 1994). Lung explants were harvested at 24 and 48 h, fixed in 4% paraformaldehyde and processed for whole mount in situ hybridization.

In situ hybridization

All cDNA clones used for probe labeling were from NIA Mouse 15K cDNA Clone Set, distributed by the Microarray Core Facility in Tufts University School of Medicine. The accession numbers for the cDNA clones are: *Enc1* (BG062990), *Tomm40* (BG063919), *Pa2g4* (BG064819), *Rex3* (BG064920), AK48222 (BG066249), C79329 (BG066485), AK046712 (BG066982), AK014226 (BG067751), AK035172 (BG070966), *Tgfbi* (BG072750), *Rab7* (BG074292), *Sfpg* (BG068503), *Wwp2* (BG072455), *Ptn* (BG073550), AK 003537 (BG074573), *Nfix* (BG075770); AK007899 (BG063646); The cDNA inserts with SP6 promoter region were amplified by PCR using M13 primers. The DNA templates for the following genes were generated by PCR with the primers that have either T7 or T3 promoters. The primer sequences are: *Dusp9* forward primer: 5′ - AATTAACCCTCACTAAAGG CCTGTGCTTGAGCTCTGATT-3′ , *Dusp9* backward primer: 5′ - TAATACGACTCACTATAGG GAGTGAGAGGTGAAGCTTCT-3′ ; *Timm8a* forward primer: 5′ -AATTAACCCTCACTAAAGGG CTATGGAGTGTTCCTGCAAT-3′ , *Timm8a* backward primer: 5′ -TAATACGACTCACTATAGGG ATGGAATCGATGTCTACCAT-3′ ; *CaII* forward primer: AATTAACCCTCACTAAAGGG CCATATGAAGGTAGGATAAT, *CaII* backward primer: TAATACGACTCACTATAGGG ATTGTGTTGTGGTATGTTAT; *Srp20* forward primer: AATTAACCCTCACTAAAGGG CAGAGCTATTGTAACGTCT, *Srp20* backward primer: TAATACGACTCACTATAGGG GACTTGATACCAAGCTCAC; *Slc4a1* forward primer: AATTAACCCTCACTAAAGGG GAACTAGAACTTGTGAGAGA, *Slc4a1* backward primer: TAATACGACTCACTATAGGG ACAGACACGTTTATTGGCAA. PCR products were purified and used as template for probe labeling. DIG-labeled RNA probes were generated using the appropriate RNA polymerase, as described on the manufacturer's manual (Ambion). The quality of labeled RNA probes was assessed by gel electrophoresis. Whole mount in situ hybridization of freshly isolated E9.5–13 lungs or lung cultures was performed in 96-well plates as previously described (Wertz and Herrmann, 2000).

Western blotting

Protein extracts from trachea and proximal regions of cultured lung explants (control, all-trans-RA 10^{-6} M; $n = 4$ for each condition) were loaded for gel electrophoresis, then transferred onto nitrocellulose membrane, blocked with 5% milk in TBST and incubated overnight with RARγ antibody (rabbit polyclonal antibody, Bioreagents, 1:2000) in TBST with 5% of milk. Immuno-Star HRP Chemiluminescent kit (Bio-rad) was used for secondary antibody reaction and signal development according to manufacturer's protocol. The membrane was stripped after RARγ detection and then re-probed with anti α-tubulin antibody (1:5000, Sigma) following the same protocol.

Results and discussion

This study was designed to characterize the differences in the transcriptional profile of the branching vs. non-branching regions of the E11.5 mouse respiratory tract. We focused on E11.5 because (1) this represents one of the earliest stages in which the respiratory and the digestive tract have been completely separated; (2) all lobes are clearly identified and branching morphogenesis has just initiated; and (3) while a P–D axis has been already defined, epithelial tubules have not undergone terminal differentiation and are still able to be re-specified, as shown by grafting studies(Ohtsuka et al., 2001; Wessells, 1970).

Validation of the array data

From the 12,500 known or predicted genes present on the array (Murine U74A v2, Affymetrix) we found 83 genes enriched in the branching region, and 128 genes enriched in non-branching region (FC > 1.75, $P < 0.05$; Tables 1 and 2). The microarray data were validated by comparing the results with published gene expression patterns in E11–12 lungs,

Table 1
Branching region-enriched genes

Accession no.	Protein encoded/homolog	Fold change	Rank	Expression pattern/reference
Cell adhesion and extracellular matrix proteins				
M62470	thrombospondin 1	2.72	15	Liu and Hogan, 2002
L19932	transforming growth factor, beta induced, 68 kDa	2.33	24	Figs. 4A–I
AJ012160	trophoblast glycoprotein	1.86	57	n.d.
AA683966	mucin and cadherin like	1.78	76	Fig. 2I
Ligand/receptor				
D85028	semaphorin 3A	7.50	3	Kagoshima and Ito, 2001
AI848841	patched, shh receptor	2.47	21	Bellusci et al., 1997
X94322	melanoma inhibitory activity	2.15	29	Lin and Shannon, 2002
AF019046	tumor necrosis factor receptor superfamily, member 11a	2.03	37	n.d.
M64849	platelet-derived growth factor B chain	1.96	45	Han et al., 1992
Transcription factors				
U84725	GATA binding protein 5	17.83	1	Morrisey et al., 1997
M26283	homeobox B5	6.52	4	Holland and Hogan, 1988
M61007	CCAAT/enhancer binding protein (C/EBP), beta	4.93	5	n.d.
M98502	zinc finger protein 46	3.65	7	n.d.
M18401	homeobox B6	3.35	8	Holland and Hogan, 1988
X95503	pleiomorphic adenoma gene-like 1	2.64	16	n.d.
X63190	ets variant gene 4 (E1A enhancer binding protein, E1AF)	2.50	19	Liu and Hogan, 2002
L35949	HNF-3/forkhead homolog 8	2.35	22	Peterson et al., 1997
AB009693	v-maf musculoaponeurotic fibrosarcoma oncogene family, protein G (avian)	2.08	34	n.d.
U79550	snail homolog 2 (*Drosophila*)	1.99	42	Savagner et al., 1998
M12731	neuroblastoma myc-related oncogene 1	1.80	71	Moens et al., 1992
D87908	nuclear protein 95	1.77	79	n.d.
AK035172	zinc finger, DHHC domain containing 6 (*Zdhhc6*)	1.77	78	Fig. 2M
Retinoic related				
AA790008	reduced expression 3 (*Rex3*)	2.35	23	Fig. 2O
Proteolysis				
AI838669	proteasome 26S subunit, non-ATPase, 12	2.49	20	n.d.
AI838853	ubiquitin carboxyl-terminal esterase L5	2.31	25	n.d.
U43918	proliferation-associated 2G4, 38 kDa (*Pa2g4*)	2.01	39	Fig. 2F
AW120683	cell division cycle 34 homolog	1.82	67	n.d.
Ion channel				
AV374320	similar to solute carrier family 4, sodium bicarbonate cotransporter, member 7	11.13	2	n.d.
X02677	solute carrier family 4 (anion exchanger), member 1 (*Slc4a1*)	1.83	64	Fig. 2P
Cytoskeleton proteins				
AB011678	doublecortin	2.61	17	n.d.
X60671	villin 2	2.01	38	n.d.
AA184423	ectodermal-neural cortex 1 (*Enc1*)	1.96	46	Fig. 2E
U72519	Ena-vasodilator stimulated phosphoprotein	1.89	54	n.d.
AA867778	actinin, alpha 1	1.84	61	n.d.
Cell cycle regulators				
AA756292	chromosome condensation 1	2.14	30	n.d.
X57800	proliferating cell nuclear antigen	1.84	59	n.d.
AI173038	chromatin assembly factor 1, subunit B	1.84	62	n.d.
AA856349	protein regulator of cytokinesis 1	1.81	70	n.d.
Metabolic enzymes				
M25944	carbonic anhydrase 2 (*CaII*)	2.84	12	Fig. 2Q
AJ238213	exonuclease 1	2.21	27	n.d.
Y11666	hexokinase 2	2.13	31	n.d.
AW122030	phosphoserine aminotransferase	2.13	32	n.d.
M14223	ribonucleotide reductase M2	2.00	40	n.d.
U49350	cytidine 5′-triphosphate synthase	1.81	69	n.d.
AF059735	C-terminal binding protein 2	1.77	77	n.d.

Table 1 (*continued*)

Accession no.	Protein encoded/homolog	Fold change	Rank	Expression pattern/reference
Metabolic enzymes				
AF031486	spermine synthase	1.75	83	n.d.
Kinase/phosphatase				
AA285446	dual specificity phosphatase 9 (*Dusp9*)	2.75	14	Fig. 2G
M96163	serum-inducible kinase	2.60	18	n.d.
AI845584	dual specificity phosphatase 6	1.88	55	n.d.
GTPase signal pathway				
AW123750	guanine nucleotide binding protein, gamma 2 subunit	2.82	13	n.d.
AW124226	GTP-binding protein Sara	2.07	35	n.d.
X02452	Kirsten rat sarcoma oncogene 2, expressed	1.84	63	n.d.
X89650	RAB7, member RAS oncogene family	1.79	74	Fig. 2H
AK14226	dedicator of cytokinesis 7 (*Dock7*)	2.06	36	Fig. 2L
Splicing factor				
AW123909	RNA binding protein gene with multiple splicing	1.87	56	n.d.
X53824	splicing factor, arginine/serine-rich 3 (*Sfrs3*)	1.85	58	Fig. 2D
AW060546	splicing factor proline/glutamine rich (*Sfpq*)	1.76	82	Fig. 2C
Hemoglobin				
J00413	hemoglobin, beta adult major chain	1.97	44	n.d.
X14061	hemoglobin Y, beta-like embryonic chain	1.92	48	n.d.
M13125	hemoglobin X, alpha-like embryonic chain in Hba complex	1.79	75	n.d.
V00714	hemoglobin alpha, adult chain 1	1.77	81	n.d.
Others				
AA921489	surfactant associated protein C	3.33	9	Wert et al., 1993
U44088	pleckstrin homology-like domain, family A, member 1	3.02	11	n.d.
D85904	heat shock protein 4	2.21	26	n.d.
AA655369	translocase of inner mitochondrial membrane 8 homolog a (yeast) (*Timm8a*)	1.99	41	Fig. 2B
AF062378	calmodulin binding protein 1	1.97	43	n.d.
AF093853	antioxidant protein 2	1.92	47	n.d.
AW050268	HLA-B associated transcript 2	1.92	49	n.d.
AW048763	NMDA receptor-regulated gene 1	1.91	50	n.d.
AI843178	cerebellar postnatal development protein 1	1.90	51	n.d.
AW047032	protein (peptidyl-prolyl cis/trans isomerase) NIMA-interacting 1	1.90	52	n.d.
AF043249	translocase of outer mitochondrial membrane 40 homolog (yeast) (*Tomm40*)	1.90	53	Fig. 2A
ESTs				
AK48222	4921526G09Rik	4.27	6	Fig. 2N
AV242583	2410002F01Rik	3.07	10	n.d.
AV334517	2010012D11Rik	2.17	28	n.d.
U21906	U21906	2.10	33	n.d.
AI122538	2810417H13Rik	1.84	60	n.d.
AW120606	Flana-pending	1.82	65	n.d.
C79329	C79329	1.82	66	Fig. 2J
AI853476	2610312E17Rik	1.82	68	n.d.
AK046712	B430320C24Rik	1.80	72	Fig. 2K
AW121031	D11Ertd175e	1.79	73	n.d.
AI847972	D130027G05Rik	1.77	80	n.d.

n.d. = not described.

and by performing whole mount in situ hybridization of the genes whose expression in the lung had not previously characterized.

The majority of the genes identified in our survey had not been formerly described in the embryonic lung. We found that only 15% of the transcripts (13 out of 83) enriched in the branching region were previously reported in the distal lung (Table 1 and references therein). These included the distal lung marker *Surfactant protein C* (*Sp-C*) (Wert et al., 1993), the transcription factors *Pcna* (*proliferating cell nuclear antigen*), N-*myc*, *Foxf1a*, *Hoxb5* and *b6*, *GATA5*, *Etv4(Pea3)* and *Snai*l (*slug*) (Holland and Hogan, 1988; Lim et al., 2002; Liu and Hogan, 2002; Moens et al., 1992; Morrisey et al., 1997; Savagner et al., 1998), the signaling molecules *Patched* (receptor of *Shh*), *Semaphorin 3A*, *platelet-derived growth factor B* and the extracellular glycoprotein *thrombospondin 1*

Table 2
Non-branching region-enriched genes

Accession No.	Protein encoded/homolog	Fold change	Rank	Expression pattern/reference
Cell adhesion and extracellular matrix proteins				
D00613	matrix gamma-carboxyglutamate (gla) protein	4.41	11	Luo et al., 1995
X78445	astrotactin 1	3.71	13	n.d.
X56304	tenascin C	3.58	15	n.d.
M60523	osteoblast specific factor 2 (fasciclin I-like)	2.55	38	n.d.
D13664	vascular cell adhesion molecule 1	2.43	46	n.d.
D82029	cadherin 6	2.19	57	n.d.
AA763466	procollagen, type I, alpha 1	2.10	63	n.d.
AW212495	procollagen, type IX, alpha 3	2.06	66	n.d.
X58251	procollagen, type I, alpha 2	2.06	69	n.d.
Z18272	procollagen, type VI, alpha 2	1.94	81	n.d.
L07803	thrombospondin 2	1.85	95	Iruela-Arispe et al., 1993
U69176	laminin, alpha 4	1.81	103	n.d.
AF101164	CEA-related cell adhesion molecule 2	1.80	108	n.d.
AB024538	immunoglobulin superfamily containing leucine-rich repeat	1.77	119	n.d.
AA919594	elastin	2.91	26	n.d.
AW124007	matrilin 4	2.56	37	n.d.
L38971	integral membrane protein 2A	2.39	47	n.d.
AK003537	1110007F23Rik	2.26	52	Fig. 3A
M84487	odd Oz/ten-m homolog 3 (*Drosophila*)	2.12	60	n.d.
X75285	fibulin 2	1.91	87	Zhang et al., 1996
AB025413	odd Oz/ten-m homolog 4 (*Drosophila*)	1.86	91	n.d.
X53928	biglycan	1.79	111	n.d.
AA838868	latent transforming growth factor beta binding protein 4	1.78	118	Sterner-Kock, et al., 2002
Ligand and receptor				
M89798	wingless-related MMTV integration site 5A (*Wnt5a*)	11.24	1	Li et al., 2002
D90225	pleiotrophin	3.20	20	Vanderwinden et al., 1992; Fig. 3C
AW125442	protein kinase inhibitor, alpha	2.97	25	n.d.
AI504074	G protein-coupled receptor 97	2.76	31	n.d.
U42467	leptin receptor	2.59	34	n.d.
D50086	neuropilin	2.23	54	Kagoshima and Ito, 2001
L12030	chemokine (C-X-C motif) ligand 12, beta	2.19	56	n.d.
L47480	bone morphogenetic protein 4	2.11	61	Weaver et al., 2003
L12029	chemokine (C-X-C motif) ligand 12, alpha	2.06	67	n.d.
AF014117	glial cell line derived neurotrophic factor family receptor alpha 1	2.06	68	n.d.
D31951	osteoglycin	1.92	82	n.d.
L38580	galanin	1.92	83	n.d.
D13903	protein tyrosine phosphatase, receptor type, D	1.88	89	n.d.
X80764	tyrosine kinase receptor 1	1.85	94	Taichman et al., 2003
U41341	S100 calcium binding protein A11 (calizzarin)	1.82	100	n.d.
U72634	unc5 homolog (*C. elegans*) 3	1.77	122	n.d.
Transcription factor				
X74040	forkhead box C2	5.49	4	n.d.
M63649	twist gene homolog, (*Drosophila*)	5.23	6	n.d.
U48721	Zinc finger protein 60	2.83	27	n.d.
AF035717	transcription factor 21	2.61	33	Quaggin et al., 1999
U20282	transcription factor 20	2.52	39	n.d.
X94127	SRY-box containing gene 2	2.46	43	n.d.
Z97062	Sin3-associated polypeptide 18	2.45	45	n.d.
AW048640	inhibitor of DNA binding 3	2.17	58	n.d.
D70849	zinc finger protein of the cerebellum 3	2.14	59	n.d.
AJ010605	SRY-box containing gene 6	2.11	62	n.d.
U03873	paired related homeobox 1	2.09	64	n.d.
AF047389	SRY-box containing gene 10	2.07	65	n.d.
AI849939	5830413E08Rik	2.04	70	n.d.
U61362	transducin-like enhancer of split 1, homolog of *Drosophila* E (spl)	1.92	84	n.d.
AI837107	single-stranded DNA binding protein 2	1.83	97	n.d.
AI603944	B230354B21Rik	1.83	98	n.d.
Y07688	nuclear factor I/X	1.80	106	Fig. 3B
AI840267	sirtuin 2 homolog (*S. cerevisiae*)	1.80	109	n.d.
U92704	early B-cell factor 3	1.78	115	n.d.

Table 2 (*continued*)

Accession No.	Protein encoded/homolog	Fold change	Rank	Expression pattern/reference
Transcription factor				
L27453	pre B-cell leukemia transcription factor 1	1.76	126	n.d.
Retinoic acid related				
M34476	retinoic acid receptor, gamma	5.36	5	Mollard et al., 2000b
X15789	cellular retinoic acid binding protein I	4.61	8	n.d.
AF062476	stimulated by retinoic acid gene 6	3.34	17	n.d.
AJ001616	myeloid-associated differentiation marker	1.91	86	n.d.
X95281	retinal short-chain dehydrogenase/reductase 1	1.75	127	n.d.
Proteolysis				
AJ131851	cathepsin F	8.95	3	n.d.
AA921411	WW domain-containing protein 2 (*Wwp2*)	3.20	19	Figs. 5A–H
AI844932	F-box only protein 8	2.83	28	n.d.
AB025412	fibroblast activation protein	2.27	51	n.d.
AF077738	carboxypeptidase X 1 (M14 family)	1.95	80	n.d.
Z12604	matrix metalloproteinase 11	1.85	93	n.d.
J03520	plasminogen activator, tissue	1.77	120	n.d.
U48797	bone morphogenetic protein 1	1.75	128	Fukagawa et al., 1994
Ion channel				
X81202	glycine receptor, beta subunit	1.95	79	n.d.
AF004666	solute carrier family 8 (sodium/calcium exchanger), member 1	1.92	85	n.d.
AV278013	solute carrier family 4, sodium bicarbonate cotransporter, member 7	1.87	90	n.d.
AF047838	chloride channel calcium activated 1	1.86	92	Gandhi et al., 1998
AF012871	potassium voltage-gated channel, subfamily H, member 2	1.81	102	n.d.
Cytoskeleton proteins				
AV251191	filaggrin	9.92	2	n.d.
M83985	synaptosomal-associated protein, 91 kDa	4.66	7	n.d.
D85923	myosin heavy chain 11, smooth muscle	4.51	9	n.d.
U28932	calponin 1	3.63	14	Tollet et al., 2001
M15501	actin, alpha, cardiac	3.15	23	Tollet et al., 2001
AV213431	troponin T1, skeletal, slow	3.05	24	n.d.
X13297	actin, alpha 2, smooth muscle, aorta	2.47	41	n.d.
Z68618	transgelin	2.01	75	n.d.
AI641895	shroom	1.96	77	n.d.
L47600	troponin T2, cardiac	1.95	78	n.d.
AI849075	capping protein (actin filament), gelsolin-like	1.82	101	n.d.
Cell cycle regulators				
L12447	insulin-like growth factor binding protein 5	2.56	36	van Kleffens et al., 1999
Y12474	centrin 3	2.20	55	n.d.
X65128	growth arrest specific 1	2.03	74	Lee et al., 2001
Metabolic enzymes				
U92702	cytochrome P450, 1b1, benz[a]anthracene inducible	4.38	12	n.d.
AI854020	cysteine dioxygenase 1, cytosolic	3.16	21	n.d.
AW048512	enoyl Coenzyme A hydratase, short chain, 1, mitochondrial	1.85	96	n.d.
AF011336	ATPase, class II, type 9A	1.83	99	n.d.
AF023463	phytanoyl-CoA hydroxylase	1.76	125	n.d.
GTPase signal pathway				
AJ007971	interferon-inducible GTPase	3.16	22	n.d.
AW121127	ras homolog gene family, member J	2.45	44	n.d.
U96634	Rho guanine nucleotide exchange factor (GEF7)	1.80	104	n.d.
AB020741	Nik related kinase	1.80	107	n.d.
Others				
D21165	visinin-like 1	3.41	16	n.d.
L04961	inactive X specific transcripts	2.80	29	n.d.
AA980164	SPARC related modular calcium binding 2	2.77	30	n.d.
M14044	annexin A2	2.58	35	n.d.

(*continued on next page*)

Table 2 (*continued*)

Accession No.	Protein encoded/homolog	Fold change	Rank	Expression pattern/reference
Others				
U59282	F1F0 ATP synthase E subunit	2.46	42	n.d.
U13371	kidney cell line derived transcript 1	2.03	73	Tymms et al., 1997
AB026808	synaptotagmin 11	2.01	76	n.d.
U12566	Defensin related cryptdin, related sequence 12	1.80	105	n.d.
Y08361	reversion induced LIM gene	1.78	112	n.d.
X78989	testis derived transcript	1.78	116	n.d.
AJ001633	annexin A3	1.76	123	n.d.
AF027707	Bcl-2-related ovarian killer protein	1.76	124	n.d.
ESTs				
AV305843	1110062M06Rik	4.44	10	n.d.
AI842065	AI842065	3.21	18	n.d.
AA518586	5530400H20Rik	2.68	32	n.d.
AV376312	4930422J18Rik	2.49	40	n.d.
AI596360	4930422J18Rik	2.37	48	n.d.
AA260139	Emu2-pending	2.30	49	n.d.
AW124049	D5Ertd593e	2.29	50	n.d.
AV366654	1110007F23Rik	2.26	53	n.d.
AW045417	1110007H17Rik	2.04	71	n.d.
AI851387	5830436L09Rik	2.04	72	n.d.
AI843106	1110002G11Rik	1.89	88	n.d.
Y10007	1500041O16Rik	1.79	110	n.d.
AW046101	D8Ertd594e	1.78	113	n.d.
AI853573	AI853573	1.78	114	n.d.
AW125223	2410002J21Rik	1.78	117	n.d.
AA575098	D930018N21Rik	1.77	121	n.d.

n.d. = not described.

(Bellusci et al., 1997; Han et al., 1992; Kagoshima and Ito, 2001; Liu and Hogan, 2002).

For the transcripts enriched in the non-branching region, 13% (17 out of 128) had already been reported in proximal lung (Table 2 and references therein). These included the transcription factors *Pod1* (*zinc finger protein 21*), *Rarγ*, *Wnt5a*, and *pleiotrophin* and its receptor (*protein tyrosine phosphatase*, *receptor type*, *D*)(Li et al., 2002; Lohnes et al., 1993a; Mollard et al., 2000b; Quaggin et al., 1999; Vanderwinden et al., 1992), the cell adhesion molecules *thrombospondin 2* and *Gla*; and cytoskeleton molecules such as *Calponin 1*, *Cardiac alpha actin* (Iruela-Arispe et al., 1993; Luo et al., 1995; Tollet et al., 2001).

By in situ hybridization we confirmed proximal expression of four out of the five uncharacterized genes from the non-branching region, and distal expression of 18 out of 19 uncharacterized genes from the branching region. The overall agreement of our array data with published expression patterns and in situ hybridization results suggested that this approach reliably detects regional differences in gene expression in the E11.5 lung.

Factors influencing the outcome of the array data

We asked whether the proportion of epithelial to mesenchymal cells was markedly different in proximal and distal regions to bias the interpretation of the array data. This did not seem to be the case, since epithelial cytokeratins (*Endo A* and *Endo B*) and mesenchymal *vimentin* genes were not differentially enriched in any of the regions ($P = 0.69$ for *Endo A*; $P = 0.52$ for *Endo B*; $P = 0.26$ for *vimentin*). Moreover, in situ hybridization analysis showed that mesenchymal and epithelial genes were well represented in the gene lists from both regions.

We used the GoMiner Bioinformatics tool to find the representation of GO biological process categories in the gene lists originated from our screen (Zeeberg et al., 2003). We found that the category associated with cell cycle and cell proliferation was the sole category overrepresented in the branching region. This was consistent with the increased proliferation activity of the distal lung. Analysis of the gene list from the non-branching region revealed that the categories overrepresented were associated with catalytic and proteolytic activities, smooth muscle formation and muscle contraction, extracellular matrix deposition, cell motility, extracellular matrix and cell adhesion (all at $P < 0.01$). These reflect the specific developmental events that occur in the more morphogenetically stable proximal regions. The low number of categories overrepresented in the distal region was somewhat surprising, since progenitor cells in the distal lung are expected to be more diverse and, thus, activate multiple genetic pathways. Presumably these genes could not be consistently detected by the microarray because

their expression levels were too low or because they may have been restricted to a small population of cells. For example, *Fgf10* transcripts were not detectable in our array. *Bmp4*, which is dynamically expressed in distal epithelium and in proximal and distal mesenchyme, was found enriched in proximal samples(Weaver et al., 2003).

Identification of genes differentially expressed in the branching region

In situ hybridization analysis of the 18 previously uncharacterized genes enriched in the branching region revealed three major patterns of transcript distribution.

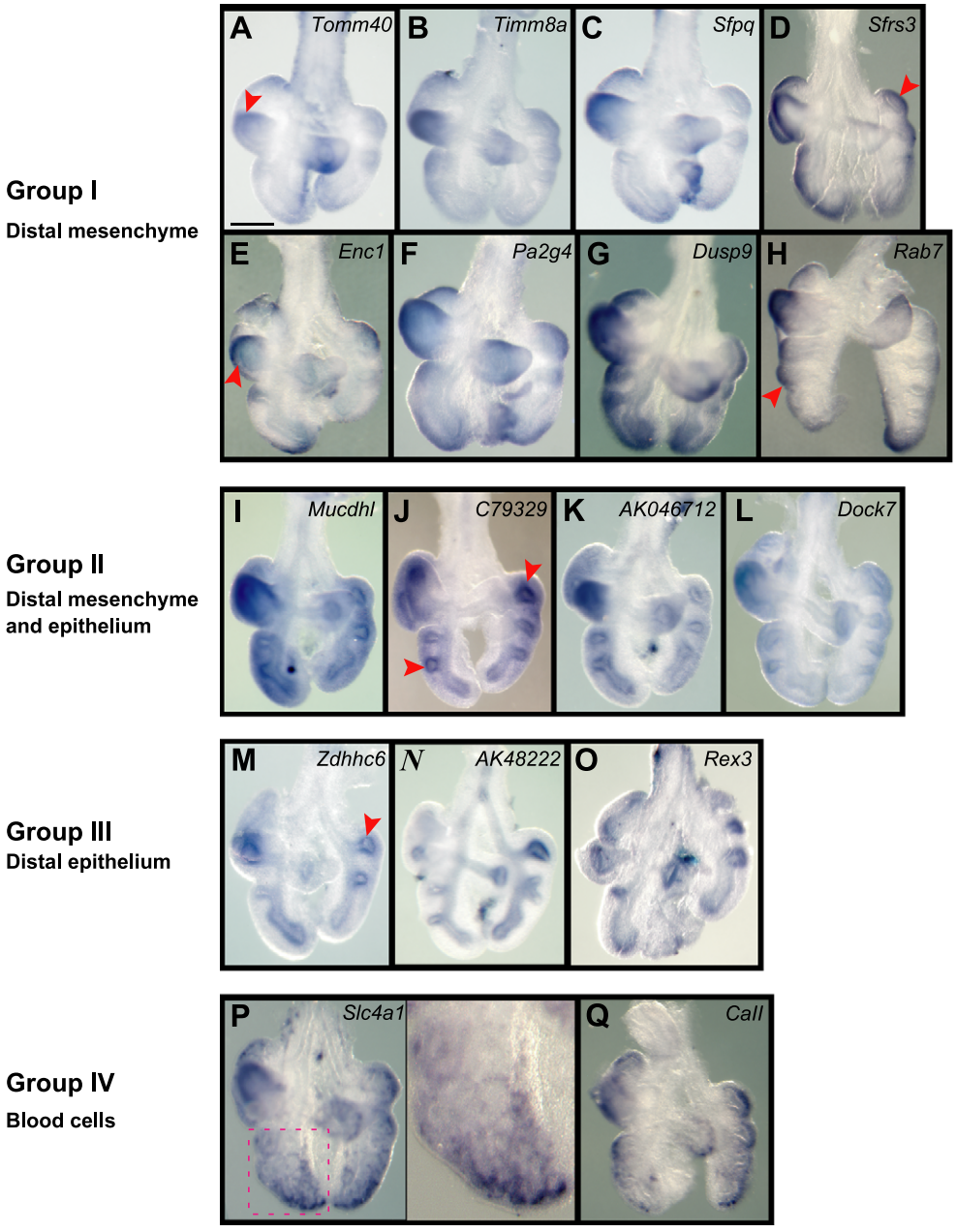

Fig. 2. Expression pattern of genes enriched in branching region (arrowheads) of E11.5 mouse lung by whole mount in *situ* hybridization (ISH). Group I consisted of genes expressed in the distal mesenchyme: (A) *translocase of outer mitochondrial membrane 40 homolog* (*Tomm40*); (B) *translocase of inner mitochondrial membrane 8 homolog a* (*Timm8a*); (C) *splicing factor proline/glutamine rich* (*Sfpq*); (D) *splicing factor, arginine/serine-rich 3* (*Srp20* or *Sfrs3*); (E) *ectodermal-neural cortex 1* (*Enc1*); (F) *proliferation-associated 2G4, 38 kDa* (*Pa2g4*); (G) *dual specificity phosphatase 9* (*Dusp9*); (H) *Rab7, member RAS oncogene family* (*Rab7*). Group II represents the genes expressed in both distal mesenchyme and epithelium: (I) *mucin and cadherin like* (*Mucdhl*); (J) EST (C79329); (K) EST (AK046712); (L) *dedicator of cytokinesis 7* (*Dock7*). Group III are distal epithelial-specific genes: (M) *zinc finger, DHHC domain containing 6* (*Zdhhc6*); (N) EST (AK48222); (O) *reduced expression 3* (*Rex3*). Group IV includes genes expressed in blood cells: (P) *solute carrier family 4* (*anion exchanger*), *member 1* (*Slc4a1*, see also high magnification on the right); (Q) *carbonic anhydrase 2* (*CaII*). Scale bar in A represents 250 μM.

Group I consisted of genes expressed solely in the distal mesenchyme. There were eight genes in this group: two translocases (*Tomm40* and *Timm8a*), two splicing factors (*Sfpq* and *Sfrs3*), *Enc1*, *Pa2g4*, *Dusp9* and *Rab7*.

Tomm40 (*translocase of outer mitochondrial membrane 40 homolog*) (Suzuki et al., 2000) and *Timm8a* (*translocase of inner mitochondrial membrane 8 homolog*) are mouse gene homologous of two yeast translocases(Figs. 2A and B). *Timm8a* is mutated in Deafness Dystonia Syndrome (MTS/DFN-1); its interaction with Signal Transduction Adaptor Molecule-1 (STAM1) has been reported. STAM1 is involved in cytokine signaling activity by interacting with Janus kinase (Blackstone et al., 2003; Roesch et al., 2002). The restricted expression of two members of this family in overlapping domains of the distal mesenchyme is intriguing and suggests a potential role in intracellular transport of proteins.

Sfpq (*splicing factor proline/glutamine rich*) is a nuclear protein with multiple functions, including RNA splicing, transcriptional regulation and tumorigenesis (Fig. 2C) (Shav-Tal and Zipori, 2002). *Sfsr3* (*similar to Splicing factor*, *arginine/serine-rich 3*, also known as *Srp20*) has multiple roles in regulating constitutive and alternative splicing in vivo (Fig. 2D). *Sfsr3* homozygous null mutant embryos fail to form blastocysts, indicating the essential role of this gene during the initial stages of mouse development (Jumaa et al., 1999).

Enc1 (*ectodermal-neural cortex 1*) is an actin-binding protein with Kelch domain known to be up-regulated by p53 in colorectal cancers and by the *beta-catenin/TCF* pathways in HeLa cells (Fig. 2E) (Fujita et al., 2001; Polyak et al., 1997). Over-expression of *Enc1* in HCT116 colon carcinoma cells results in increased tumor growth rate (Fujita et al., 2001). Based on its restricted expression in distal mesenchyme and induction by *beta-catenin/TCF*, *Enc1* is likely a candidate target of *Wnt* genes. Various *Wnt* family members have been identified in the distal lung, including *Wnt2*, *Wnt5a* (also in the proximal region), *Wnt11* and *Wnt7b*. *Wnt7b* is of particular interest because of the severe lung hypoplasia and vascular defects reported in knockout mice (Shu et al., 2002). *Wnt7b* is expressed in distal epithelial tubules and signals in the mesenchyme via the *beta-catenin/TCF* pathway to regulate mesenchymal cell proliferation and vascular differentiation (Shu et al., 2002; Tebar et al., 2001).

p38-2G4 (*proliferation-associated protein 2G4*), the gene encoding the proliferation-associated nuclear protein 38 kDa, is also restricted to the mesenchyme around distal buds (Fig. 2F). Little is known about its function. *p38-2G4* has potential methionyl aminopeptidase activity. In HeLa cells, expression of this gene is associated with specific phases of the cycle (Radomski and Jost, 1995). Its distribution in the E11.5 lung suggests a selective role in proliferating distal mesenchymal cells.

Dusp9 (*dual-specificity MAPK phosphatase-9* or *Mkp-4*) has been shown to inactivate *ERK1/2* (*extracellular signal-regulated kinase-1/2*) by de-phosphorylation (Fig. 2G) (Dickinson et al., 2002). Strong *Dusp9* mRNA expression was detected in the peripheral layers of the distal mesenchyme near newly formed buds with lower signals in the interbud region of mesenchyme. These gradients suggest a dynamic expression pattern and presumably a role in regulating activity of ERK-dependent signals, such as FGF, in the lung mesenchyme. Based on its localization *Dusp9* is likely a modulator of the *Fgf9-Fgfr2c* pathway (Colvin et al., 2001).

Rab7 (Fig. 2H, *RAB7*, *member RAS oncogene family*) is a member of the *Rab* family of GTPases and vesicle transport proteins. In *Drosophila* embryos, *rab7* is required for the establishment of the gradient of *decapentaplegic* (*dpp*) through a transcytosis process. *Dpp*, the *Drosophila* homolog of the mammalian BMP, is required for proper segmentation of *Drosophila* embryo (Entchev and Gonzalez-Gaitan, 2002). In the E11.5 lung *Rab7* could play a similar a role by controlling gradients of *Bmp4*, which is expressed by distal epithelial and subepithelial mesenchymal cells (Weaver et al., 2003).

Group II includes genes expressed in both distal mesenchyme and epithelium. There are two known genes (*Mucdhl* and *Dock7*) and two ESTs (AK046712, Fig. 2K and C79329, Fig. 2J) in this group. *Mucdhl*, the *mucin and cadherin-like gene*, has been reported in fetal kidneys with different spliced isoforms (Fig. 2I) (Goldberg et al., 2002). *Dock7* (*dedicator of cytokinesis 7*) encodes a DOCK180-related protein with guanine nucleotide exchange activity (Fig. 2L). *Dock180* is upstream of the small GTPase *Rac* and has been implicated in *Rac*-dependent phagocytosis and cell migration in *C. elegans*. *Dock180* (*Dock1*) is also involved in cell migration and invasion in COS-7 cells (Grimsley et al., 2004). *Dock7* may have a similar role in controlling cell movements during distal lung morphogenesis.

Group III consisted of genes with expression restricted to the distal epithelium. *Zdhhc6*, *Rex3* and an EST (AK48222) (Figs. 2M–O) are representative of this group. *Zdhhc6* (*zinc finger*, *DHHC domain containing 6*) is a novel transcription factor with DHHC-type zinc finger domain. *Rex3* (*reduced expression 3*) is also known as *Bex1* (*brain expressed X-linked 1*) and shares homologous sequences with *Bex2* and *Bex3*. *Bex3*, also known as *nerve growth factor receptor associated protein*1, plays a role in nerve growth factor-induced apoptosis (Mukai et al., 2003). *Rex3* is of particular interest because of its regulation by RA (Faria et al., 1998), and will be discussed subsequently. Expression of these genes is likely to be dynamic as the architecture of distal epithelial structures rapidly changes during branching.

An additional group (group IV), which included *CaII* (*carbonic anhydrase 2*) and *Slc4a1* (*solute carrier family 4*, *member 1*) (Figs. 2P and Q), represented the genes expressed by blood cells. These genes were enriched in the branching region, likely due to blood cell trapping in the highly vascular distal lung.

Identification of genes differentially expressed in the non-branching region

We determined the spatial distribution of four transcripts enriched in the non-branching region. In situ hybridization revealed a broad, homogenous distribution of transcripts throughout the proximal lung and trachea for all genes (*Nfix*, *Ptn* and AV230893) but one (*Wwp2*).

Nfix (*nuclear factor I/X*) is a CAAT box binding transcription factor from the *Nuclear Factor I* (*NFI*) family (Fig. 3B). Members of this family regulate a variety of other genes with very diverse functions. For example, *Renin*, a regulator of arterial blood pressure, is one of the Nfix targets (Pan et al., 2004).

Wwp2 (*WW domain-containing protein 2*) encodes a Nedd4-like ubiquitin-protein ligase. *Nedd4* expression has been reported in proliferating and prehypertrophic chondrocytes during skeletal development (Weston and Underhill, 2000); however, no information about *Wwp2* is currently available. We found that *Wwp2* transcripts were restricted to a specific region in the ventral–lateral mesenchyme of the trachea and the main bronchi (Fig. 3D and 5). The similarity of the *Wwp2* pattern with that of *Rarγ* in this region (Mollard et al., 2000b) suggested that *Wwp2* could be involved in local regulation of RA signaling. We selected *Wwp2* as a candidate gene for further studies (see below).

Tgfbi is a potential mediator of the TGFβ1 effects in the branching region

Our array analysis revealed *Tgfbi* (βig-h3, *TGF beta induced*), a gene that encodes a cell adhesion-extracellular matrix protein, significantly enriched in the branching region. By in situ hybridization we found *Tgfbi* expression restricted to the stalk region of distal buds (Fig. 4C). This localization was consistent with a role in suppressing local budding. The absence of signals in morphogenetically more stable proximal regions suggested that *Tgfbi* mediated responses and occur only in areas that are actively branching (Fig. 4C). Although expression of *Tgfbi* in the embryonic lung and other organs had been reported, no systematic analysis of its expression pattern in developing airways, and its relationship to local signaling was available.

To gain additional insights into the developmental expression and regulation of *Tgfbi* by TGFβ1, we extended our analysis to lungs at early stages in vivo and to cultured lung explants. We found *Tgfbi* transcripts in the lung mesenchyme as early as E9.5–10, when primary buds are forming. In primary lung buds, expression was excluded from the mesenchyme surrounding the tips (Fig. 4A). Later at E10.5, *Tgfbi* transcripts were localized to regions flanking the nascent secondary buds (Fig. 4B). This dynamic pattern in regions immediately proximal to newly formed buds continues through E11–12, and was also observed in lung cultures (Figs. 4C, D–I).

Previous studies have shown that in the E11–12 lung *Tgfβ1* is transcribed in the subepithelial mesenchyme, throughout its anterior–posterior axis (Lebeche et al., 1999; Schmid et al., 1991). However, TGFβ1 protein is accumulated in epithelial–mesenchymal interfaces of the stalks and clefts (Heine et al., 1990), sites where we found *Tgfbi* mRNA expression.

Culturing E11.5 lung explants with exogenous TGFβ1 (10–50 ng/ml) resulted in distal expansion of the *Tgfbi* mRNA expression domain within 24 h (Fig. 4D right and F). By 48 h, TGFβ1 treatment markedly inhibited lung growth and branching (Serra et al., 1994), and resulted in diffuse up-regulation of *Tgfbi* in the distal mesenchyme (Figs. 4G–I). The widespread distribution of *Tgfbi* transcripts in TGFβ1-treated explants suggested that in the normal lung, endogenous gradients of TGFβ1 restrict *Tgfbi* transcription to the stalk region of distal buds during branching. Whether this represents a direct or an indirect effect in gene transcription we could not determine based in our results. Culturing E11.5 lung with cyclohexamide, to inhibit protein synthesis, markedly affected the viability of the explants and reproducibility of the results (data not shown).

Tgfbi has been shown to mediate some of the TGFβ1-related effects in biological processes. These include tumor suppression, apoptosis and promotion of cell adhesion (Kim et al., 2003; Zhao et al., 2002a,b, 2003). Studies in cell lines suggest that, depending on the cell type, TGFβ1 may either induce or prevent apoptosis (Horowitz et al., 2004). For

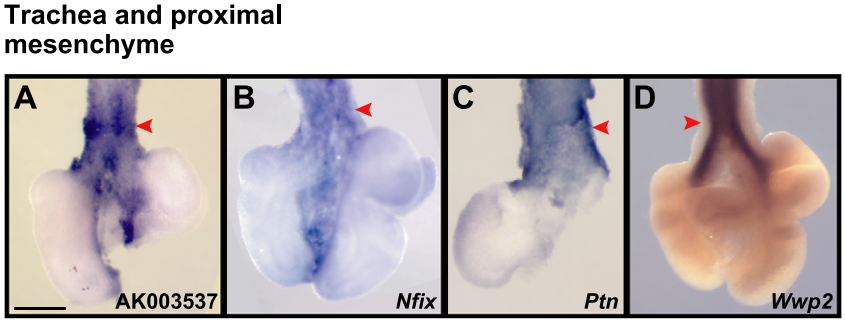

Fig. 3. Expression patterns of genes enriched in the non-branching region (arrowheads) by whole mount ISH. (A) AK003537; (B) *nuclear factor I/X* (*Nfix*); (C) *pleiotrophin* (*Ptn*); (D) *WW domain-containing protein 2* (*Wwp2*). Scale bar in A represents 250 μM.

example, in lung fetal mesenchymal cells IMR90, which express high levels of *Tgfbi*, TGFβ1 signaling prevents cell death. Interestingly, during early branching, apoptosis is found predominantly in cleft mesenchymal cells (Levesque et al., 2000). This suggests that activation of the *Tgfβ1-Tgfbi* pathway may help to maintain a balance between apoptotic

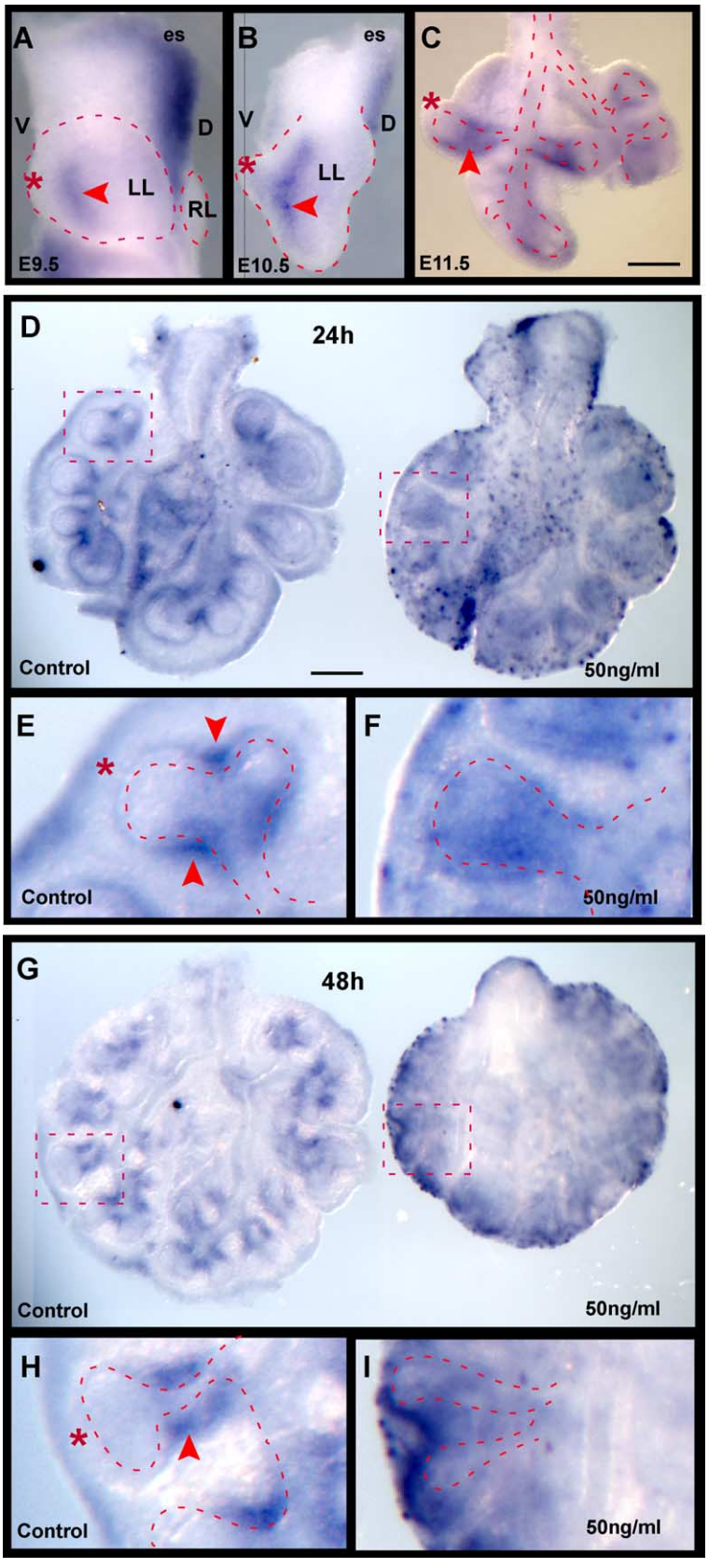

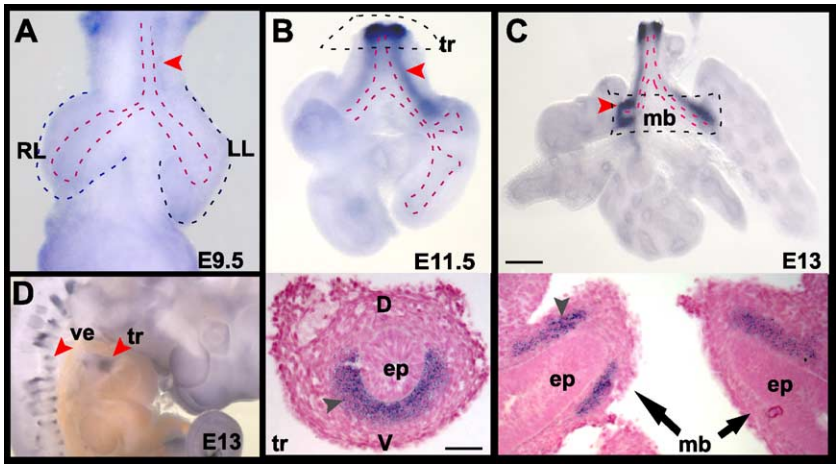

Fig. 5. Expression pattern of *Wwp2* in developing respiratory tract and vertebrate. (A) Low levels of expression of *Wwp2* (arrowhead) were first observed at E9.5 in mesenchymal cells adjacent to the tracheal epithelium. (B) At E11.5 and (C) E13, *Wwp2* signals were clearly seen in mesenchymal cells of ventral–lateral regions of trachea and main bronchi, where cartilage primordium will form. Fast Red staining of sections from specimens in B and C (low panel) at the level of trachea (tr) and main bronchi (mb) (areas outlined in black) confirmed this pattern. (D) *Wwp2* is also expressed in cartilage primordia of developing vertebrate (ve) in the E13 embryo. Dashed lines outline the outer surface (blue in A) and epithelium (red in A–C) of the respiratory tract. RL, right lung; LL, left lung; tr, trachea; mb, main bronchi; D, dorsal; V, ventral; ep, epithelium; ve, vertebrate; Scale bar in C and D represents 150 and 30 μM, respectively.

and non-apoptotic signals, perhaps favoring the latter. In epithelial cell lines, *Tgfbi* appears to function as a tumor suppressor gene, since its down-regulation has been associated with a tumorigenic phenotype (Zhao et al., 2002a,b, 2003). As a mediator of cell matrix interactions, *Tgfbi* has been shown to bind to various integrins to regulate cell adhesion, migration and proliferation (Bae et al., 2002). Some of these *integrins* are present in the developing lung, where they can be critical for branching, as exemplified by α3β1 integrin (Kreidberg et al., 1996). Taken together, these suggest that *Tgfbi* may be a local modulator of cell growth and presumably cell survival in specific regions of branching tubules.

Components of the RA pathway and RA targets were enriched in the proximal region

Studies using a *RARE lacZ* reporter mouse have shown that branching morphogenesis is characterized by down-regulation of retinoid signaling in distal but not in proximal regions of respiratory tract (Malpel et al., 2000; Mollard et al., 2000a). In our screen, we found several known components of the RA signaling pathway and RA responsive genes differentially enriched in the non-branching region, where RA is maintained active; for example *Rarγ*, *cellular RA binding protein I* (*Crabp1*), *stimulated by RA gene 6* (*Stra6*), *myeloid-associated differentiation marker* (*Myadm*) and *retinal short chain dehydrogenase reductase 1* (Tables 1 and 2; Bouillet et al., 1997; Cui et al., 2001; Rattner et al., 2000).

Retinoid-related genes were underrepresented in the branching region. The only RA targets enriched in this region were either those, such as *Hoxb5* and *Hoxb6*, 5′ genes with low responsiveness to RA, which likely do not require RA to maintain their expression in the lung (Tables 1 and 2), or genes, such as *Rex3*, whose expression is down-regulated by RA signaling. *Rex3* was first described in F9 murine teratocarcinoma cells as a gene whose transcription is inhibited by retinoic acid (Faria et al., 1998). In the E11.5 lung, the presence of *Rex3* in the distal epithelium likely resulted from the local loss of RA activity. This could be part of a mechanism that allows further development of distal buds.

An ubiquitin ligase potentially associated with Rarγ is differentially expressed in the non-branching region of the respiratory tract

In eukaryotes, activation of ubiquitin/proteasome-mediated proteolysis allows controlled degradation of regulatory molecules, including RARs. Ubiquitination is carried out by at least three classes of enzymes: ubiquitin-activating (E1), -conjugating (E2) and -protein ligases (E3) enzymes (Ciechanover et al., 2000).

Fig. 4. Expression and regulation of *Tgfbi* mRNA in the developing lung. (A) At E9.5, *Tgfbi* is expressed in the ventral mesenchyme of primary lung buds (arrowheads); signals are excluded from distal sites, where secondary buds will form (asterisks); strong signal are also present in esophagus (es). (B) At E10.5, *Tgfbi* signals are restricted to the proximal mesenchyme of newly formed secondary buds. (C) At E11.5, *Tgfbi* is seen in mesenchymal cells that surround the stalk of distal lung buds. (D–F) Cultured E11.5 lung at 24 h shows the typical *Tgfbi* expression pattern in mesenchymal cells adjacent to stalk of distal buds (D, left and E); treatment with TGFβ-1 (50 ng/ml) disrupts the localized expression pattern of *Tgfbi* and expands *Tgfbi* expression domain to distal location (D, right and F). (G–I) By 48 h, the change of *Tgfbi* pattern induced by TGFβ-1 became more evident. E, F, H and I are enlarged views of the outlined region in D and G. LL, left lung; RL, right lung; V, ventral; D, dorsal; es, esophagus. Scale bar in C and D represents 175 and 225 μM, respectively.

One of the most interesting findings of our screen was the restricted expression of *Wwp2*, a gene encoding a *Nedd4-like ubiquitin ligase* in proximal regions of the E11.5 respiratory tract. The ventral and ventral–lateral pattern of transcript distribution in tracheal and proximal lung mesenchyme was highly similar to that described for *Rarγ*. This became clearer when we analyzed lungs from E9.5 to E13.5 embryos (Figs. 5A–C) and when we found *Wwp2* transcripts in extra pulmonary *Rarγ*-expressing sites, such as the vertebral column (Fig. 5D).

Studies in keratinocytes, COS 1 and F9 cells indicate that ubiquitin-mediated proteolysis regulates endogenous levels of RARγ (Kopf et al., 2000). Moreover, there is evidence that, at least in some of these cells, RA induces expression of enzymes of the ubiquitin pathway for RARγ degradation (Kitareewan et al., 2002). This prompted us to investigate the RA regulation of *Wwp2* transcription and its relationship to Rar γ expression in our system. We cultured E11.5 lungs from a *RARE lacZ* reporter mouse up to 72 h with RA (10^{-6} to 10^{-5} M) or BMS 493 (10^{-6} M)-containing media to enhance or inhibit retinoid signaling, respectively (Mollard et al., 2000a; Malpel et al., 2000). Efficacy of treatment was confirmed by monitoring *lacZ* expression in these cultures (Malpel et al., 2000; Rossant et al., 1991, data not shown). Unexpectedly, we found that endogenous RA is not required for *Wwp2* transcription in proximal airways, since antagonizing RA signaling did not affect *Wwp2* expression (Figs. 6A–C). In turn, exogenous RA significantly reduced *Wwp2* transcription in a concentration-dependent manner in proximal airways (Figs. 6D, E).

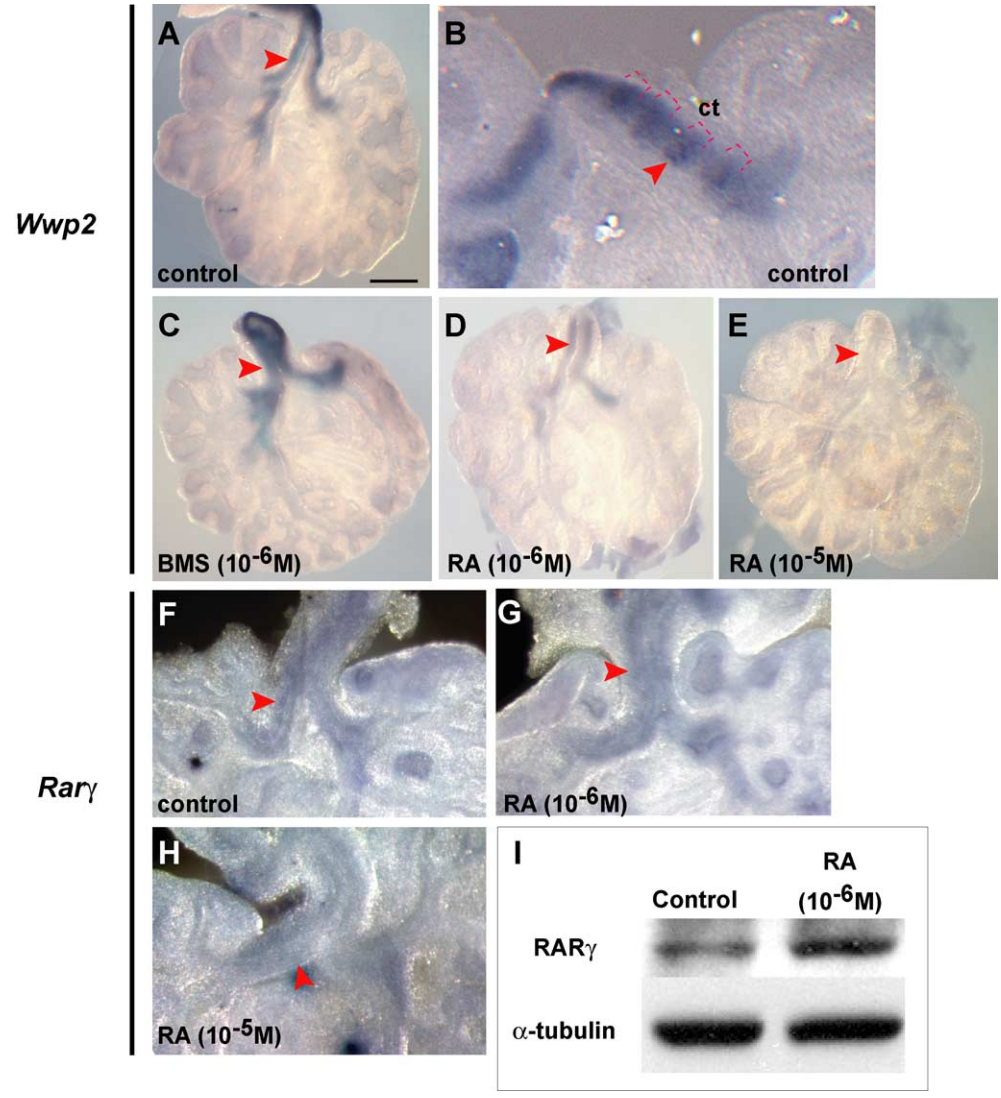

Fig. 6. Expression of *Wwp2* and RARγ in lung cultures. RA down-regulated *Wwp2* expression and increased RARγ protein level in cultured lungs. (A and B) In 48-h control lung cultures, *Wwp2* signals continue to be expressed at sites of precartilage formation (ct). (C) BMS treatment has no effect on *Wwp2* expression. (D and E) Expression of *Wwp2* is significantly down-regulated by RA (10^{-5} to 10^{-6} M) in 48-h cultured lungs. (F) In control cultures, *Rarγ* transcripts are expressed in the mesenchyme of the trachea and main bronchi similarly as *Wwp2*. (G and H) RA treatment of lung cultures does not alter the level and distribution of *Rarγ* mRNA. (I) Western blot analysis shows that RARγ protein levels in the proximal region of cultured explants are increased by RA treatment. ct, cartilage precursor. Scale bar in A represents 150 μM.

To determine whether these treatments had an impact in RARγ protein or transcripts levels, we performed in situ hybridization and Western blot analysis of tracheal and main bronchi regions isolated from these cultures. Figs. 6F–H confirmed data from previous studies in cell lines, which showed that RA does not induce *Rarγ* transcription (Boudjelal et al., 2002; Yamamoto et al., 2000). We found, however, that levels of RARγ protein were increased in RA treated cultures, as compared to controls (Fig. 6I). The most likely explanation is that RARγ protein became more stable with the down-regulation of *Wwp2 expression*. This suggests that, under physiological conditions, *Wwp2*-mediated proteolysis contributes to regulate endogenous levels of RARγ protein in the proximal mesenchyme.

The biological relevance of this observation resides in the fact that the sites where we found *Wwp2* expression corresponded to the regions where *Rarγ* is critical for the development of cartilage primodium in the respiratory tract and vertebrae (Figs. 5D and I). Cartilage progenitor cells require tightly controlled RARγ signaling for proper development. Deletion of the *Rarγ* gene in mice results in defects in tracheal cartilage ring and anterior axial skeleton (Lohnes et al., 1993). Moreover, there is in vivo and in vitro evidence that RARγ is critical to mediate RA teratogenesis and to induce expression of the RA-metabolizing enzyme, *Cyp26a1*, when levels of RA increase to supra-physiological levels (Abu-Abed et al., 1998). We have previously shown that under similar conditions, RA treatment of E11.5 explants induces ectopic *Cyp26a1* expression in the tracheal and proximal lung mesenchyme (Malpel et al., 2000). Interestingly, these are essentially the same sites where we found *Rarγ* and *Wwp2* transcribed. We propose that down-regulation of *Wwp2* mRNA and induction of *Cyp26a1* gene expression by inappropriately high levels of RA may be part of a local mechanism that controls RA signaling and its effects in this region. Our model predicts that inhibition of *Wwp2* expression by excess RA prevents normal RARγ degradation. This ensures that there will be enough RARγ available to mediate the RA teratogenic responses and to induce *Cyp26a1*, as an attempt to lower RA levels.

Concluding remarks

In summary, we provide the molecular signature of the branching and non-branching regions of the E11.5 mouse respiratory tract. The transcriptional profiles reported here provide insights into the global trends in gene expression associated with the developmental events that are typical of these regions. At E11.5 the distal lung is characterized by high branching activity, increased growth of both epithelial and mesenchymal compartments, and plasticity of distal progenitor cells. We found 83 genes enriched in the distal region. Many of these genes were associated with cell proliferation or had a potential link with local known regulatory pathways, such as the FGF or Wnt. Other genes, such as splicing factors and translocases, for which we had no previous information about their role in the distal lung, could represent, or be part of novel pathways to be investigated. Our profiling revealed 128 genes enriched in the proximal respiratory tract region. These included SRY transcription factors, BMPs, RA-related genes and a large number of extracellular matrix genes. Several of these genes have been associated with morphogenetic stability and formation of proximal mesenchymal derivatives, such as tracheal cartilage primordia and smooth muscle layers. In some cases we found representative members of the same gene family differentially expressed in each region. This was the case of *thrombospondins 1* and *2*, respectively, at distal and proximal sites.

The use of stringent criteria for gene selection and the complex cellular composition of the samples in our survey limited our ability to retrieve all important components of these networks. However, the validity and power of our approach in identifying potentially relevant genes for further functional analysis was well supported by our results. Consistent with this, we confirmed the majority of the selected genes at the expected location by in situ hybridization, and we could identify all major patterns of transcript distribution for both regions. Moreover, our screen was able to uncover genes, such as *Tgfbi* and *Wwp2*, localized to specific subpopulations of cells, where they are likely regulating specific developmental events. The database generated here also represents a valuable resource for comparisons with similar databases from embryonic kidney, salivary gland and other branching structures to identify common regulatory mechanisms.

Acknowledgments

We thank Lan Wei in the Microarray Core Facility of Tufts University for providing us the cDNA clones and PCR products. We thank Jerome Brody, Avrum Spira, Felicia Chen and Tushar Desai for critical reading of the manuscript. We are also grateful to Xiaoqian Qi for technical assistance. This work was supported by grants from NIH/NHLBI RO-1 HL/HD67129-01, and NIH/NHLBI (PO1 HL47049).

References

Abu-Abed, S.S., Beckett, B.R., Chiba, H., Chithalen, J.V., Jones, G., Metzger, D., Chambon, P., Petkovich, M., 1998. Mouse P450RAI (CYP26) expression and retinoic acid-inducible retinoic acid metabolism in F9 cells are regulated by retinoic acid receptor gamma and retinoid X receptor alpha. J. Biol. Chem. 273, 2409–2415.

Bae, J.S., Lee, S.H., Kim, J.E., Choi, J.Y., Park, R.W., Yong, P.J., Park, H.S., Sohn, Y.S., Lee, D.S., Bae, L.E., Kim, I.S., 2002. Betaig-h3 supports keratinocyte adhesion, migration, and proliferation through alpha3beta1 integrin. Biochem. Biophys. Res. Commun. 294, 940–948.

Bellusci, S., Furuta, Y., Rush, M.G., Henderson, R., Winnier, G., Hogan, B.L., 1997. Involvement of Sonic hedgehog (Shh) in mouse embryonic lung growth and morphogenesis. Development 124, 53–63.

Blackstone, C., Roberts, R.G., Seeburg, D.P., Sheng, M., 2003. Interaction of the deafness-dystonia protein DDP/TIMM8a with the signal transduction adaptor molecule STAM1. Biochem. Biophys. Res. Commun. 305, 345–352.

Boudjelal, M., Voorhees, J.J., Fisher, G.J., 2002. Retinoid signaling is attenuated by proteasome-mediated degradation of retinoid receptors in human keratinocyte HaCaT cells. Exp. Cell Res. 274, 130–137.

Bouillet, P., Sapin, V., Chazaud, C., Messaddeq, N., Decimo, D., Dolle, P., Chambon, P., 1997. Developmental expression pattern of Stra6, a retinoic acid-responsive gene encoding a new type of membrane protein. Mech. Dev. 63, 173–186.

Butler, M.J., Jacobsen, T.L., Cain, D.M., Jarman, M.G., Hubank, M., Whittle, J.R., Phillips, R., Simcox, A., 2003. Discovery of genes with highly restricted expression patterns in the *Drosophila* wing disc using DNA oligonucleotide microarrays. Development 130, 659–670.

Cardoso, W.V., 2001. Molecular regulation of lung development. Annu. Rev. Physiol. 63, 471–494.

Ciechanover, A., Orian, A., Schwartz, A.L., 2000. Ubiquitin-mediated proteolysis: biological regulation via destruction. Bioessays 22, 442–451.

Colvin, J.S., White, A.C., Pratt, S.J., Ornitz, D.M., 2001. Lung hypoplasia and neonatal death in Fgf9-null mice identify this gene as an essential regulator of lung mesenchyme. Development 128, 2095–2106.

Cui, W., Yu, L., He, H., Chu, Y., Gao, J., Wan, B., Tang, L., Zhao, S., 2001. Cloning of human myeloid-associated differentiation marker (MYADM) gene whose expression was up-regulated in NB4 cells induced by all-trans retinoic acid. Mol. Biol. Rep. 28, 123–138.

Dickinson, R.J., Williams, D.J., Slack, D.N., Williamson, J., Seternes, O.M., Keyse, S.M., 2002. Characterization of a murine gene encoding a developmentally regulated cytoplasmic dual-specificity mitogen-activated protein kinase phosphatase. Biochem. J. 364, 145–155.

Entchev, E.V., Gonzalez-Gaitan, M.A., 2002. Morphogen gradient formation and vesicular trafficking. Traffic 3, 98–109.

Faria, T.N., LaRosa, G.J., Wilen, E., Liao, J., Gudas, L.J., 1998. Characterization of genes which exhibit reduced expression during the retinoic acid-induced differentiation of F9 teratocarcinoma cells: involvement of cyclin D3 in RA-mediated growth arrest. Mol. Cell. Endocrinol. 143, 155–166.

Fujita, M., Furukawa, Y., Tsunoda, T., Tanaka, T., Ogawa, M., Nakamura, Y., 2001. Up-regulation of the ectodermal-neural cortex 1 (ENC1) gene, a downstream target of the beta-catenin/T-cell factor complex, in colorectal carcinomas. Cancer Res. 61, 7722–7726.

Fukagawa, M., Suzuki, N., Hogan, B.L., Jones, C.M., 1994. Embryonic expression of mouse bone morphogenetic protein-1 (BMP-1), which is related to the *Drosophila* dorsoventral gene tolloid and encodes a putative astacin metalloendopeptidase. Dev. Biol. 163, 175–183.

Gandhi, R., Elble, R.C., Gruber, A.D., Schreur, K.D., Ji, H.L., Fuller, C.M., Pauli, B.U., 1998. Molecular and functional characterization of a calcium-sensitive chloride channel from mouse lung. J. Biol. Chem. 273, 32096–32101.

Goldberg, M., Wei, M., Tycko, B., Falikovich, I., Warburton, D., 2002. Identification and expression analysis of the human mu-protocadherin gene in fetal and adult kidneys. Am. J. Physiol.: Renal Physiol. 283, F454–F463.

Grimsley, C.M., Kinchen, J.M., Tosello-Trampont, A.C., Brugnera, E., Haney, L.B., Lu, M., Chen, Q., Klingele, D., Hengartner, M.O., Ravichandran, K.S., 2004. Dock180 and ELMO1 proteins cooperate to promote evolutionarily conserved Rac-dependent cell migration. J. Biol. Chem. 279, 6087–6097.

Han, R.N., Mawdsley, C., Souza, P., Tanswell, A.K., Post, M., 1992. Platelet-derived growth factors and growth-related genes in rat lung: III. Immunolocalization during fetal development. Pediatr. Res. 31, 323–329.

Heine, U.I., Munoz, E.F., Flanders, K.C., Roberts, A.B., Sporn, M.B., 1990. Colocalization of TGF-beta 1 and collagen I and III, fibronectin and glycosaminoglycans during lung branching morphogenesis. Development 109, 29–36.

Hogan, B.L., 1999. Morphogenesis. Cell 96, 225–233.

Holland, P.W., Hogan, B.L., 1988. Spatially restricted patterns of expression of the homeobox-containing gene Hox 2.1. during mouse embryogenesis. Development 102, 159–174.

Horowitz, J.C., Lee, D.Y., Waghray, M., Keshamouni, V.G., Thomas, P.E., Zhang, H., Cui, Z., Thannickal, V.J., 2004. Activation of the pro-survival phosphatidylinositol 3-kinase/AKT pathway by transforming growth factor-beta1 in mesenchymal cells is mediated by p38 MAPK-dependent induction of an autocrine growth factor. J. Biol. Chem. 279, 1359–1367.

Iruela-Arispe, M.L., Liska, D.J., Sage, E.H., Bornstein, P., 1993. Differential expression of thrombospondin 1, 2, and 3 during murine development. Dev. Dyn. 197, 40–56.

Jumaa, H., Wei, G., Nielsen, P.J., 1999. Blastocyst formation is blocked in mouse embryos lacking the splicing factor SRp20. Curr. Biol. 9, 899–902.

Kagoshima, M., Ito, T., 2001. Diverse gene expression and function of semaphorins in developing lung: positive and negative regulatory roles of semaphorins in lung branching morphogenesis. Genes Cells 6, 559–571.

Kim, J.E., Kim, S.J., Jeong, H.W., Lee, B.H., Choi, J.Y., Park, R.W., Park, J.Y., Kim, I.S., 2003. RGD peptides released from beta ig-h3, a TGF-beta-induced cell-adhesive molecule, mediate apoptosis. Oncogene 22, 2045–2053.

Kitareewan, S., Pitha-Rowe, I., Sekula, D., Lowrey, C.H., Nemeth, M.J., Golub, T.R., Freemantle, S.J., Dmitrovsky, E., 2002. UBE1L is a retinoid target that triggers PML/RARalpha degradation and apoptosis in acute promyelocytic leukemia. Proc. Natl. Acad. Sci. U. S. A. 99, 3806–3811.

Kopf, E., Plassat, J.L., Vivat, V., de The, H., Chambon, P., Rochette-Egly, C., 2000. Dimerization with retinoid X receptors and phosphorylation modulate the retinoic acid-induced degradation of retinoic acid receptors alpha and gamma through the ubiquitin-proteasome pathway. J. Biol. Chem. 275, 33280–33288.

Kreidberg, J.A., Donovan, M.J., Goldstein, S.L., Rennke, H., Shepherd, K., Jones, R.C., Jaenisch, R., 1996. Alpha 3 beta 1 integrin has a crucial role in kidney and lung organogenesis. Development 122, 3537–3547.

Lebeche, D., Malpel, S., Cardoso, W.V., 1999. Fibroblast growth factor interactions in the developing lung. Mech. Dev. 86, 125–136.

Lee, K.K., Leung, A.K., Tang, M.K., Cai, D.Q., Schneider, C., Brancolini, C., Chow, P.H., 2001. Functions of the growth arrest specific 1 gene in the development of the mouse embryo. Dev. Biol. 234, 188–203.

Levesque, B.M., Vosatka, R.J., Nielsen, H.C., 2000. Dihydrotestosterone stimulates branching morphogenesis, cell proliferation, and programmed cell death in mouse embryonic lung explants. Pediatr. Res. 47, 481–491.

Li, C., Xiao, J., Hormi, K., Borok, Z., Minoo, P., 2002. Wnt5a participates in distal lung morphogenesis. Dev. Biol. 248, 68–81.

Lim, L., Kalinichenko, V.V., Whitsett, J.A., Costa, R.H., 2002. Fusion of lung lobes and vessels in mouse embryos heterozygous for the forkhead box f1 targeted allele. Am. J. Physiol.: Lung Cell. Mol. Physiol. 282, L1012–L1022.

Lin, S., Shannon, J.M., 2002. Microarray analysis of gene expression in the embryonic lung. Chest 121, 80S–81S.

Liu, Y., Hogan, B.L., 2002. Differential gene expression in the distal tip endoderm of the embryonic mouse lung. Gene Expression Patterns 2, 229–233.

Lohnes, D., Kastner, P., Dierich, A., Mark, M., LeMeur, M., Chambon, P., 1993. Function of retinoic acid receptor gamma in the mouse. Cell 73, 643–658.

Luo, G., D'Souza, R., Hogue, D., Karsenty, G., 1995. The matrix Gla protein gene is a marker of the chondrogenesis cell lineage during mouse development. J. Bone Miner. Res. 10, 325–334.

Malpel, S., Mendelsohn, C., Cardoso, W.V., 2000. Regulation of retinoic acid signaling during lung morphogenesis. Development 127, 3057–3067.

Mariani, T.J., Reed, J.J., Shapiro, S.D., 2002. Expression profiling of the developing mouse lung: insights into the establishment of the extracellular matrix. Am. J. Respir. Cell Mol. Biol. 26, 541–548.

Moens, C.B., Auerbach, A.B., Conlon, R.A., Joyner, A.L., Rossant, J., 1992. A targeted mutation reveals a role for N-myc in branching morphogenesis in the embryonic mouse lung. Genes Dev. 6, 691–704.

Mollard, R., Dziadek, M., 1998. A correlation between epithelial proliferation rates, basement membrane component localization patterns, and morphogenetic potential in the embryonic mouse lung. Am. J. Respir. Cell Mol. Biol. 19, 71–82.

Mollard, R., Ghyselinck, N.B., Wendling, O., Chambon, P., Mark, M., 2000a. Stage-dependent responses of the developing lung to retinoic acid signaling. Int. J. Dev. Biol. 44, 457–462.

Mollard, R., Viville, S., Ward, S.J., Decimo, D., Chambon, P., Dolle, P., 2000b. Tissue-specific expression of retinoic acid receptor isoform transcripts in the mouse embryo. Mech. Dev. 94, 223–232.

Morrisey, E.E., Ip, H.S., Tang, Z., Lu, M.M., Parmacek, M.S., 1997. GATA-5: a transcriptional activator expressed in a novel temporally and spatially-restricted pattern during embryonic development. Dev. Biol. 183, 21–36.

Mukai, J., Suvant, P., Sato, T.A., 2003. Nerve growth factor-dependent regulation of NADE-induced apoptosis. Vitam. Horm. 66, 385–402.

Ohtsuka, N., Urase, K., Momoi, T., Nogawa, H., 2001. Induction of bud formation of embryonic mouse tracheal epithelium by fibroblast growth factor plus transferrin in mesenchyme-free culture. Dev. Dyn. 222, 263–272.

Pan, L., Jones, C.A., Glenn, S.T., Gross, K.W., 2004. Identification of a novel region in the proximal promoter of the mouse renin gene critical for expression. Am. J. Physiol Renal. Physiol. 286, F1107–F1115.

Peterson, R.S., Lim, L., Ye, H., Zhou, H., Overdier, D.G., Costa, R.H., 1997. The winged helix transcriptional activator HFH-8 is expressed in the mesoderm of the primitive streak stage of mouse embryos and its cellular derivatives. Mech. Dev. 69, 53–69.

Polyak, K., Xia, Y., Zweier, J.L., Kinzler, K.W., Vogelstein, B., 1997. A model for p53-induced apoptosis. Nature 389, 300–305.

Quaggin, S.E., Schwartz, L., Cui, S., Igarashi, P., Deimling, J., Post, M., Rossant, J., 1999. The basic-helix-loop-helix protein pod1 is critically important for kidney and lung organogenesis. Development 126, 5771–5783.

Radomski, N., Jost, E., 1995. Molecular cloning of a murine cDNA encoding a novel protein, p38-2G4, which varies with the cell cycle. Exp. Cell Res. 220, 434–445.

Rattner, A., Smallwood, P.M., Nathans, J., 2000. Identification and characterization of all-*trans*-retinol dehydrogenase from photoreceptor outer segments, the visual cycle enzyme that reduces all-*trans*-retinal to all-*trans*-retinol. J. Biol. Chem. 275, 11034–11043.

Roesch, K., Curran, S.P., Tranebjaerg, L., Koehler, C.M., 2002. Human deafness dystonia syndrome is caused by a defect in assembly of the DDP1/TIMM8a-TIMM13 complex. Hum. Mol. Genet. 11, 477–486.

Rossant, J., Zirngibl, R., Cado, D., Shago, M., Giguere, V., 1991. Expression of a retinoic acid response element-hsplacZ transgene defines specific domains of transcriptional activity during mouse embryogenesis. Genes Dev. 5, 1333–1344.

Savagner, P., Karavanova, I., Perantoni, A., Thiery, J.P., Yamada, K.M., 1998. Slug mRNA is expressed by specific mesodermal derivatives during rodent organogenesis. Dev. Dyn. 213, 182–187.

Schmid, P., Cox, D., Bilbe, G., Maier, R., McMaster, G.K., 1991. Differential expression of TGF beta 1, beta 2 and beta 3 genes during mouse embryogenesis. Development 111, 117–130.

Serra, R., Pelton, R.W., Moses, H.L., 1994. TGF beta 1 inhibits branching morphogenesis and N-myc expression in lung bud organ cultures. Development 120, 2153–2161.

Shannon, J.M., Nielsen, L.D., Gebb, S.A., Randell, S.H., 1998. Mesenchyme specifies epithelial differentiation in reciprocal recombinants of embryonic lung and trachea. Dev. Dyn. 212, 482–494.

Shav-Tal, Y., Zipori, D., 2002. PSF and p54(nrb)/NonO—multi-functional nuclear proteins. FEBS Lett. 531, 109–114.

Shu, W., Jiang, Y.Q., Lu, M.M., Morrisey, E.E., 2002. Wnt7b regulates mesenchymal proliferation and vascular development in the lung. Development 129, 4831–4842.

Stathopoulos, A., Van Drenth, M., Erives, A., Markstein, M., Levine, M., 2002. Whole-genome analysis of dorsal–ventral patterning in the *Drosophila* embryo. Cell 111, 687–701.

Sterner-Kock, A., Thorey, I.S., Koli, K., Wempe, F., Otte, J., Bangsow, T., Kuhlmeier, K., Kirchner, T., Jin, S., Keski-Oja, J., von Melchner, H., 2002. Disruption of the gene encoding the latent transforming growth factor-beta binding protein 4 (LTBP-4) causes abnormal lung development, cardiomyopathy, and colorectal cancer. Genes Dev. 16, 2264–2273.

Suzuki, H., Okazawa, Y., Komiya, T., Saeki, K., Mekada, E., Kitada, S., Ito, A., Mihara, K., 2000. Characterization of rat TOM40, a central component of the preprotein translocase of the mitochondrial outer membrane. J. Biol. Chem. 275, 37930–37936.

Taichman, D.B., Schachtner, S.K., Li, Y., Puri, M.C., Bernstein, A., Scott, B.H., 2003. A unique pattern of Tie1 expression in the developing murine lung. Exp. Lung Res. 29, 113–122.

Tebar, M., Destree, O., de Vree, W.J., Have-Opbroek, A.A., 2001. Expression of Tcf/Lef and sFrp and localization of beta-catenin in the developing mouse lung. Mech. Dev. 109, 437–440.

Tollet, J., Everett, A.W., Sparrow, M.P., 2001. Spatial and temporal distribution of nerves, ganglia, and smooth muscle during the early pseudoglandular stage of fetal mouse lung development. Dev. Dyn. 221, 48–60.

Tymms, M.J., Ng, A.Y., Thomas, R.S., Schutte, B.C., Zhou, J., Eyre, H.J., Sutherland, G.R., Seth, A., Rosenberg, M., Papas, T., Debouck, C., Kola, I., 1997. A novel epithelial-expressed ETS gene, ELF3: human and murine cDNA sequences, murine genomic organization, human mapping to 1q32.2 and expression in tissues and cancer. Oncogene 15, 2449–2462.

Vanderwinden, J.M., Mailleux, P., Schiffmann, S.N., Vanderhaeghen, J.J., 1992. Cellular distribution of the new growth factor pleiotrophin (HB-GAM) mRNA in developing and adult rat tissues. Anat. Embryol. (Berl.) 186, 387–406.

van Kleffens, M., Groffen, C.A., Dits, N.F., Lindenbergh-Kortleve, D.J., Schuller, A.G., Bradshaw, S.L., Pintar, J.E., Zwarthoff, E.C., Drop, S.L., van Neck, J.W., 1999. Generation of antisera to mouse insulin-like growth factor binding proteins (IGFBP)-1 to -6: comparison of IGFBP protein and messenger ribonucleic acid localization in the mouse embryo. Endocrin. 140, 5944–5952.

Weaver, M., Batts, L., Hogan, B.L., 2003. Tissue interactions pattern the mesenchyme of the embryonic mouse lung. Dev. Biol. 258, 169–184.

Wert, S.E., Glasser, S.W., Korfhagen, T.R., Whitsett, J.A., 1993. Transcriptional elements from the human SP-C gene direct expression in the primordial respiratory epithelium of transgenic mice. Dev. Biol. 156, 426–443.

Wertz, K., Herrmann, B.G., 2000. Large-scale screen for genes involved in gonad development. Mech. Dev. 98, 51–70.

Wessells, N.K., 1970. Mammalian lung development: interactions in formation and morphogenesis of tracheal buds. J. Exp. Zool. 175, 455–466.

Weston, A.D., Underhill, T.M., 2000. Analysis of Nedd4 expression during skeletal development in the mouse limb. Mech. Dev. 94, 247–250.

White, K.P., Rifkin, S.A., Hurban, P., Hogness, D.S., 1999. Microarray analysis of *Drosophila* development during metamorphosis. Science 286, 2179–2184.

Yamamoto, Y., Zolfaghari, R., Ross, A.C., 2000. Regulation of CYP26 (cytochrome P450RAI) mRNA expression and retinoic acid metabolism by retinoids and dietary vitamin A in liver of mice and rats. FASEB J. 14, 2119–2127.

Zeeberg, B.R., Feng, W., Wang, G., Wang, M.D., Fojo, A.T., Sunshine, M., Narasimhan, S., Kane, D.W., Reinhold, W.C., Lababidi, S., Bussey, K.J., Riss, J., Barrett, J.C., Weinstein, J.N., 2003. GoMiner: a resource for biological interpretation of genomic and proteomic data. Genome Biol. 4, R28.

Zhang, H.Y., Timpl, R., Sasaki, T., Chu, M.L., Ekblom, P., 1996. Fibulin-1 and fibulin-2 expression during organogenesis in the developing mouse embryo. Dev. Dyn. 205, 348–364.

Zhao, Y.L., Piao, C.Q., Hei, T.K., 2002a. Downregulation of Betaig-h3

gene is causally linked to tumorigenic phenotype in asbestos treated immortalized human bronchial epithelial cells. Oncogene 21, 7471–7477.

Zhao, Y.L., Piao, C.Q., Hei, T.K., 2002b. Overexpression of Betaig-h3 gene downregulates integrin alpha5beta1 and suppresses tumorigenicity in radiation-induced tumorigenic human bronchial epithelial cells. Br. J. Cancer 86, 1923–1928.

Zhao, Y.L., Piao, C.Q., Hei, T.K., 2003. Tumor suppressor function of Betaig-h3 gene in radiation carcinogenesis. Adv. Space Res. 31, 1575–1582.